An Experimental and Numerical Study of the Effect of Microchannels Geometry on Heat Transfer of Nanofluids

Abbas N. Tuaima[1,*], Ahmed J. Shkaraha[1] , Mohammed D. Salman[1]

[1] Mechanical Department, Engineering College, Thi Qar University, Thi Qar, Iraq

ARTICLE INFO	ABSTRACT
	The use of micro-channel heat exchangers is widespread across a variety of different industrial sectors. This study presents both an experimental and a numerical analysis to compare the performance of four different designs of microchannel heat sinks. The study dealt with using pure water and nanofluid (Al2O3, CuO, and TiO2–H2O) with volumetric concentrations of (0.01- 0.03) as coolants. The software Comsol Multiphysics was employed for conducting numerical analysis in order to simulate and resolve the issue pertaining to fluid and heat flow in a three-dimensional domain. A constant heat flux of 170 kW/m^2 is applied to the lower wall of the four microchannels. The simulations were exclusively conducted within the laminar regime, covering a range of Reynolds numbers spanning from 50 to 150. The impact on the temperature of the microchannel's wall, thermal resistance, pressure drop, and friction factor is demonstrated. Based on the results obtained, it is evident that the utilization of nanofluid in the cooling process of a wavy and zigzag microchannel heat sink yields superior performance in terms of both heat transfer and dissipation, as compared to the implementation of pure water as the cooling medium for the heat sink.

1. Introduction

Systems (lTAS) in the field of biotechnology. Additionally, progress was made in the areas of Communications and Micro Devices [1-3]. The phenomenon of overheating in these gadgets is attributed to the combination of constant downsizing and uninterrupted operation. Heat dissipation is a crucial consideration in many devices or machines to prevent potential harm to specific components. Elevated temperature levels can adversely affect the efficiency and lifespan of these devices, leading to energy wastage.

Consequently, integrating an efficient cooling system into their design has become imperative[4-7]. Heat dissipation is a significant challenge in numerous engineering applications. Microchannel heat dispersants are commonly employed to mitigate thermal fluxes from electrical components. In recent years, there have been significant advancements in precise manufacturing and assembly techniques, resulting in the emergence of a thriving sector of contemporary industrial technology often known as micro-electromechanical systems (MEMS). MEMS systems have a distinct length

scale between 1 millimeter and 1 µm. The cooling fluid plays a crucial role in cooling applications since it has a substantial impact on the cooling efficiency of the device. The optimization of cooling efficiency in a microchannel heat exchanger can be attained by judiciously choosing an appropriate fluid.

Further investigation is warranted in this domain due to the proliferation of novel cooling fluids employed in recent times. The cooling systems exhibit a diverse range of geometric configurations in their microstructure, while the choice of working fluids can differ across different systems. The functionality and structural composition of the gadgets play a determining role. Hence, the categorization of cooling systems can be determined as either direct or indirect, depending on whether the operational liquid comes into direct contact with the chip or the cooling component[8-10]. The preference for liquids in cooling applications is mostly attributed to their superior thermal characteristics compared to gases. In recent times, there has been a notable concentration of researchers on the utilization and formulation of nanofluids due to their inherent benefits. Compared to conventional liquids, the superior heat transmission capability of nanofluids renders them the preferred option for coolant applications. The thermal conductivity shown by nanoparticles results in enhanced heat transfer properties.

Furthermore, it has been shown that the surface area of nanoparticles is higher in solid substances as compared to fluid molecules. Additionally, nanoparticles demonstrate a notable degree of heat conductivity. In order to enhance the turbulent motion of nanoparticles inside a fluid, it is imperative to decrease the dimensions of those nanoparticles within the range of 1-100µm [11-14].

The primary objective of this study is to conduct forced convection experiments in order to examine and analyze the thermal performance characteristics of A microchannel heat sink. Experiments were conducted to get further heat transfer data about the effectiveness of utilizing nanofluids (namely $CuOH_2O$, $Al_2O_3H_2O$, and TIO_2H_2O) as coolants compared to pure water.

2. Description of the Experimental Configuration

Figure 1 shows a schematic representation of the primary constituents of the current work's open-loop experimental facility. From the tank, the working fluid enters the annulus. When the valve is opened, pure water passes through a filter that is only utilized when the working fluid is water. The fluid temperature in the upper tank of the test unit and the inlet flow temperature are both constant. The volumetric flow rate within the open loop was measured using a flow meter. The depicted configuration of the test module that was manufactured can be observed in Figure 2. The primary components of the test section encompass a microchannel heat sink, cover plate, housing, microchannels, insulating layers, insulating block, and support plate. The geometric structure of the fabricated straight microchannel heat sink is schematically depicted in Figure 3 and Figure 4. The dimensions, which are provided in full, are summarized in Table 1. Eighteen parallel rectangular microchannels were machined into a copper (Cu) block to create the microchannel heat sink. On each side, four small holes were drilled along the centerline of the heat sink's base. Two K-type thermocouples and pressure taps were strategically placed to accurately measure the temperature increase and pressure decrease at both the inlet and outlet of the microchannel heat sink. The recorded values of all estimated quantities were documented using a digital temperature recorder.

Table 1
The dimensions of the microchannel heat sink

Wm	Lm	Hm	Hc	Wc	Lc	X
10mm	30mm	990µm	720µm	270µm	30mm	270µm
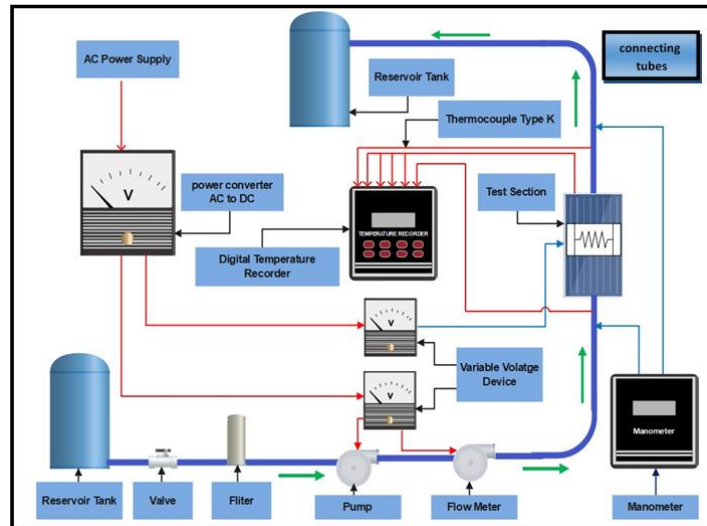
Fig. 1. displays the device is detailed schematic
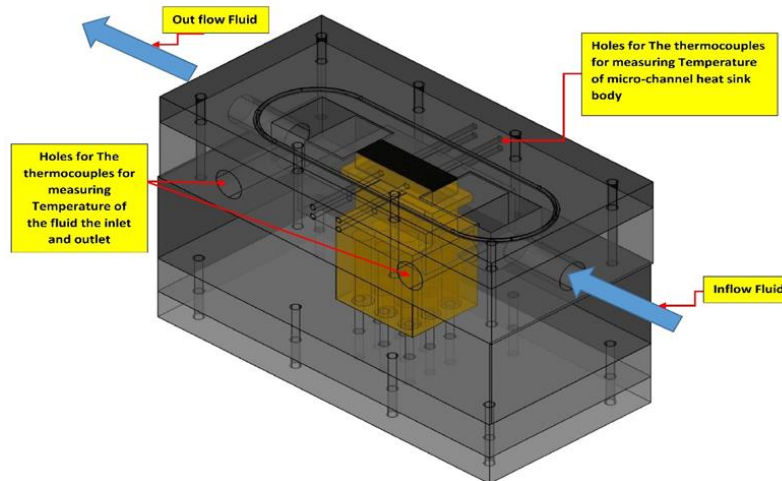
Fig. 2. Test module configuration
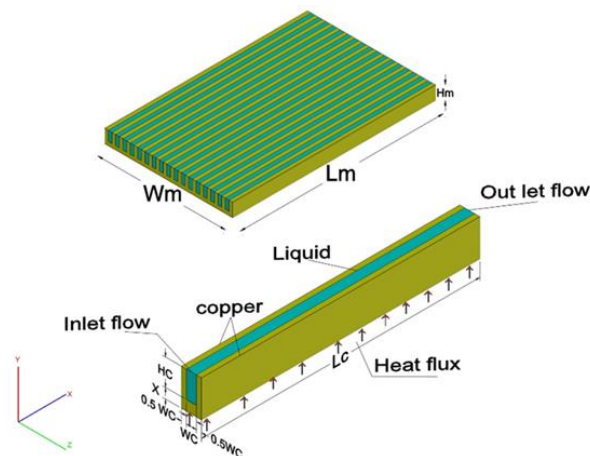
Fig. 3. Configuration for test module
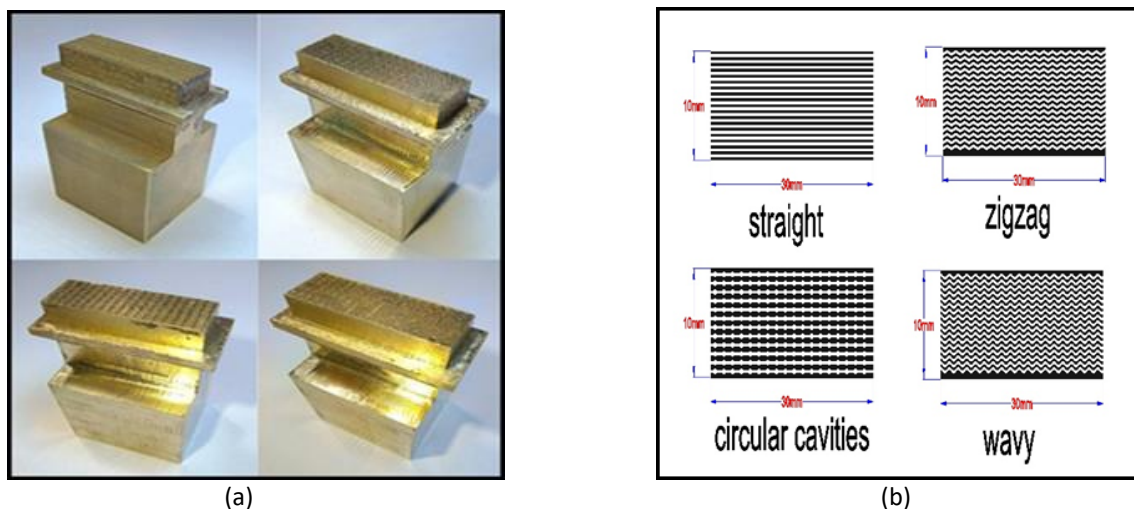
Fig. 4. (a) microchannels after manufacturing, (b) microchannels shapes used in the current work

3. The Preparation and Characterization of Nanofluids

Nanofluid is a type of fluid consisting of a basd fluid (such as water, oil, or Ethanol glycol) and nanometer-sized particles (typically less than 100 nanometers) that are homogeneously dispersed in the base fluid. Particles, typically measuring less than 100 nanometers in size, that are evenly distributed throughout the base fluid. The incorporation of nanoparticles has the potential to modify the thermo physical characteristics of the underlying fluid, including thermal conductivity, viscosity, and specific heat capacity. In this study, the utilization of nanofluids as a cooling fluid was done To enhance the thermal performance of a microchannels heat sink .In the present work, nanofluids used in this study are [(CuH$_2$O), (Al$_2$O$_3$), (Tio2)] nanofluids (see Figure 5) and used volume fractions of (0.1%, 0.2 % and 0.3% respectively) or each Nanofluid. in Table 2. The thermo-physical characteristics of nanoparticles are displayed.

Table 2
The thermophysical characteristics of nanoparticles and the Base Fluid (pure water)

Thermophysical properties	ρ (kg/m^3)	cp (J/kgK)	κ (W/mK)
Pure water (H$_2$O) [15]	997	4180	0.613
Copper oxide (CuO) [16]	6500	535.6	20
Alumina oxide (Al$_2$O$_3$) [16]	3510	497.26	1000
Titanium oxide (Ti O$_2$) [17]	4230	692	8.4

Fig. 5. Nanoparticle (CuO, Al2O3, TIO2) used in the present work

The Nano-properties needed for flow are calculated using the following equations [18, 19]:

The density value were calculated by Eq. (1):

$$(\rho cp)nf = (1-\varphi) \, \rho f + \varphi \rho f \tag{1}$$

The Specific heat value was calculated by Eq. (2)

$$cp_{nf} = \frac{\varphi(\rho cp)_p + (1-\varphi)\rho_f \, cp_f}{\rho_{nf}} \tag{2}$$

The Viscosity value was calculated by Eq. (3)

$$\mu_{nf} = \frac{\mu_f}{(1-\varphi)^{2.5}} \tag{3}$$

The Thermal conductivity value was calculated by Eq. (4)

$$\kappa_{nf} = \frac{\kappa_p + (n-1)\kappa_f - (n-1)\varphi(\kappa_f - \kappa_p)}{\kappa_p + (n-1)\kappa_f + \varphi(\kappa_f - \kappa_p)} \, \kappa_f \tag{4}$$

Where it represents (the volume of nanoparticles, cp Specific heat, μ viscosity, κ thermal conductivity, ρ the density). While the subscripts represent (nanoparticle, f base fluid, nf nanofluid).

4. Mathematical Formulation

To simplify the problem in this work and to investigate the thermal and flow characteristics of these models, there are several assumptions made about an operating condition:

i.   The flow is 3D, single-phase, Steady-state, and Laminar flow.
ii. Incompressible fluids.
iii. No Slip flow is assumed.
iv. Heat flux that is steady and uniform.
v.   The gravitational effect is negligible.
vi. Negligible radiation heat transfer.
vii. Both fluids and solids have constant thermo-physical properties.

Based on the assumptions stated above, the governing equations and boundary conditions in the Cartesian coordinates three-dimensional are the following:

The Continuity equation for the fluid [20, 21]:

$$\frac{\partial u}{\partial u} + \frac{\partial v}{\partial y} + \frac{\partial w}{\partial z} = 0 \tag{5}$$

Momentum equations (Naviers Stokes equations) can be written as:

The X-momentum equation

$$u\frac{\partial u}{\partial x} + v\frac{\partial u}{\partial y} + w\frac{\partial u}{\partial z} = -\frac{1}{\rho}\frac{\partial p}{\partial x} + \frac{\mu}{\rho}(\frac{\partial^2 u}{\partial x^2} + \frac{\partial^2 u}{\partial y^2} + \frac{\partial^2 u}{\partial z^2})$$ (6)

The Y- momentum equation

$$u\frac{\partial v}{\partial x} + v\frac{\partial v}{\partial y} + w\frac{\partial v}{\partial z} = -\frac{1}{\rho}\frac{\partial p}{\partial y} + \frac{\mu}{\rho}(\frac{\partial^2 v}{\partial x^2} + \frac{\partial^2 v}{\partial y^2} + \frac{\partial^2 v}{\partial z^2})$$ (7)

The Z- momentum equation

$$u\frac{\partial w}{\partial x} + v\frac{\partial w}{\partial y} + w\frac{\partial w}{\partial z} = -\frac{1}{\rho}\frac{\partial p}{\partial z} + \frac{\mu}{\rho}(\frac{\partial^2 w}{\partial x^2} + \frac{\partial^2 w}{\partial y^2} + \frac{\partial^2 w}{\partial z^2})$$ (8)

The energy equation for fluid and solid

$$u\frac{\partial T_f}{\partial x} + v\frac{\partial T_f}{\partial y} + w\frac{\partial T_f}{\partial z} = \frac{\kappa}{\rho C_P}(\frac{\partial^2 T_f}{\partial x^2} + \frac{\partial^2 T_f}{\partial y^2} + \frac{\partial^2 T_f}{\partial z^2})$$ (9)

In addition, the expression for the 3D solid-wall steady-state energy equation is by Eq. (10):

$$(\frac{\partial^2 T_s}{\partial x^2} + \frac{\partial^2 T_s}{\partial y^2} + \frac{\partial^2 T_s}{\partial z^2}) = 0$$ (10)

Based on Figure 6 and the previous assumptions, the following Boundary conditions are described:

i.   The temperature of a coolant fluid's inlet (Tin) is constant.
ii. The coolant fluid enters the heat sink at a constant velocity, corresponding to a Reynolds number between 200 and 1000.
iii. (a pressure outlet) is carried out Pressure gauge (0.0 pa).
iv. continuous uniform heat flux was used on the bottom wall.
v.   All the external surfaces are adiabatic.
vi. In addition, the condition was applied to ensure that the microchannel walls were non-slip.
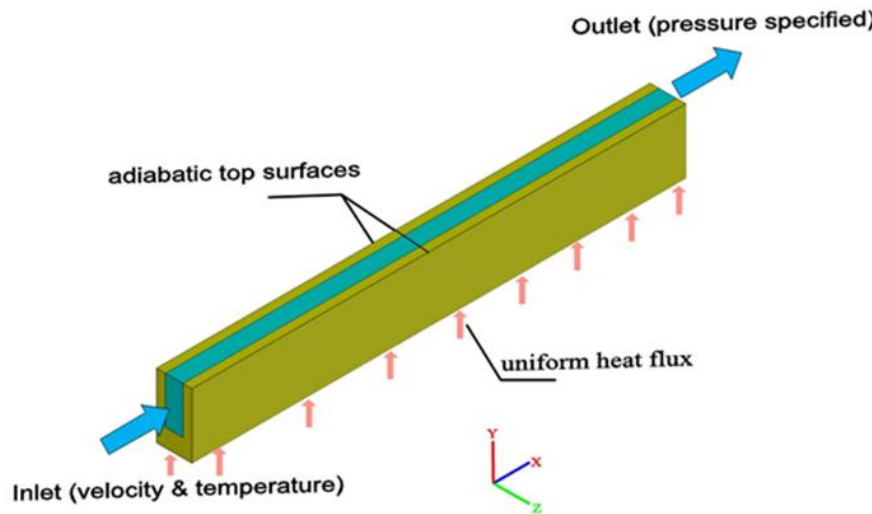
Fig. 6. The boundary conditions of the geometry

The hydraulic diameter (Dh) value was calculated by Eq. (11), [22, 23]:

$$D_h = \frac{4A}{P} = \frac{2W_S H_S}{W_S + H_S} \tag{11}$$

The Reynolds number value was calculated by Eq. (12):

$$Re = \frac{\rho\, u_{in} D_h}{\mu} \tag{12}$$

The Nusselt number value was calculated by Eq. (13), [24, 25]:

$$Nu = \frac{h D_h}{\kappa_f} \tag{13}$$

The Thermal resistance (Rth) value were calculated by Eq. (14):

$$R_{th} = \frac{T_{max} - T_{in}}{q} \tag{14}$$

The pressure drop value was calculated by Eq. (15):

$$\Delta p = \frac{2 f \rho u_{in}^2 l}{D_h} \tag{15}$$

5. Mesh Sensitivity and Validation

The grid-dependent test is initially carried out using several different mesh sizes. In order to ascertain the precision of the mesh grid, an assessment was conducted involving various .mesh types (regular, fine, finer, and extremely fine) for a straight micro-channel. Table 3 provides an explanation of the types of mesh that have been examined. Each type has a certain number of elements, domains, boundary elements, and edge elements. Table 3 provides an explanation of the types of mesh that have been examined. Each type has a certain number of elements, domains, boundary elements, and edge elements. The 'maximum temperature (Tmax) has been computed for each mesh in a straight microchannel heat sink operating at a Reynolds number of 150 and a heat flux of 170 kW/m^2. 'The obtained values have been compared. Using the following equation Eq. (16), the relative error of the desirable parameters was calculated [26]:

$$(\%) = \left| \frac{J_2 - J_1}{J_1} \right| \times 100 \tag{16}$$

Where J represents any parameter such as the Nusselt number, pressure drops, friction coefficient, and temperature, J1 and J2 represent the parameter values obtained from the finest grids and other grids, respectively.

Triangular forms were employed to achieve a high level of precision in the outcomes, as depicted in Figure 7. The simulation would involve creating three-dimensional models of the microchannel and specifying the relevant fluid and thermal properties, such as viscosity, density, thermal conductivity, and heat capacity. The software would then solve the governing equations for fluid flow and heat transfer, such as (continuity, momentum, and energy for two domains, fluid and solid).

Table 3

Mesh independent study of straight microchannel heat sink unit at Re=150, q = 170kW/m^2

Element size	Domain element	Boundary element	Edge element	Tmax (k)	Tmax error%
Extra fine	13201911	517020	8794	326	2.14
finer	3019618	176848	5270	319	1.88
fine	914715	75670	3465	313	0.319
Normal	330167	40044	2516	312	-------

(a)

(b)

(c)

(d)
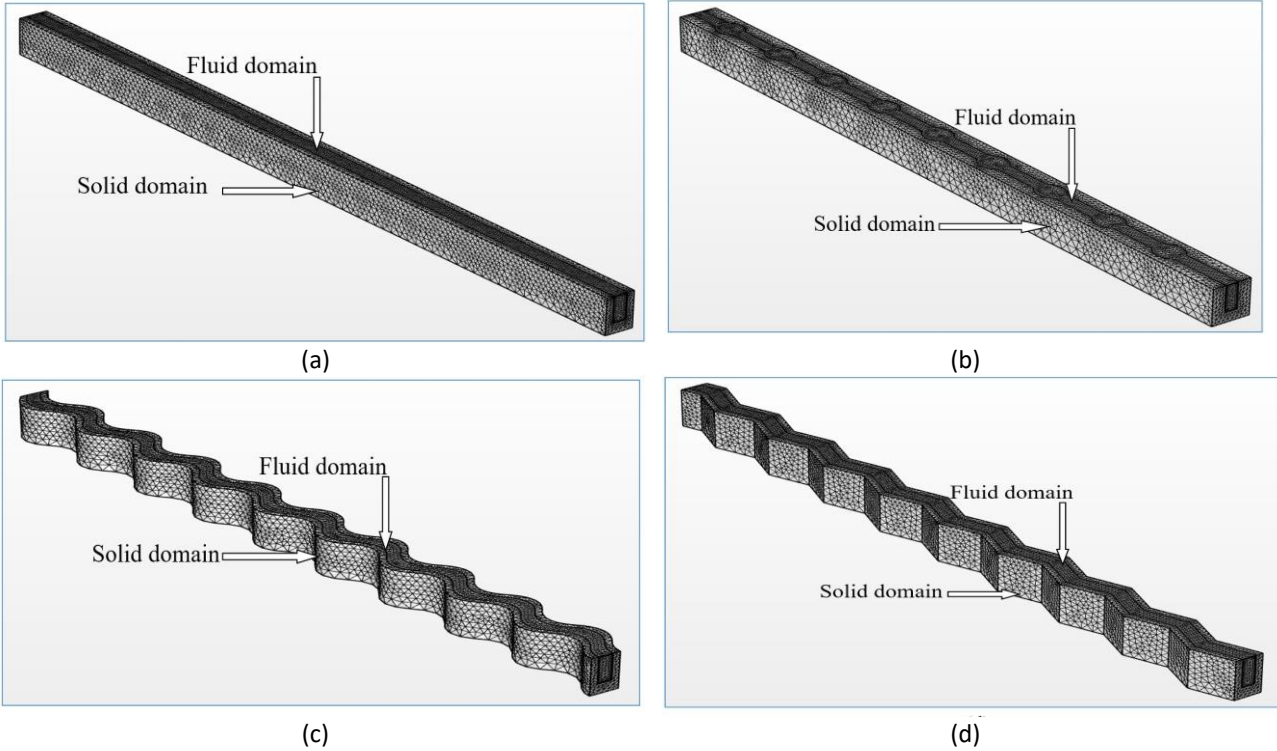
Fig. 7. Mesh distribution details for model three dimensions: (a) straight, (b) circular cavities, (c) wavy, (d) Zigzag channel

5.1 Velocity Contour Characteristics

To study the effect of shapes of microchannels (straight, Zigzag, wavy, and circular cavities) with Rectangular section entrance on velocity magnitude, and because of the similarity of observed behaviour, To reduce the quantity of illustrations, Only show one nanoparticle concentration (φ= 0.01), has been selected for Reynolds numbers Re= 150. Figure 8 show that The wavy structure increases the flow velocity compared with the other microchannel shapes used in the present work, where the way shape offers kinetic energy activity and an extra boost. As well as increased speed when using all types of nanofluids (Al$_2$O$_3$, CuO, and TiO$_2$–H$_2$O) studied. Because of that, The primary emphasis of substantial research in this topic has been on microchannel heat sinks featuring wavy shapes.
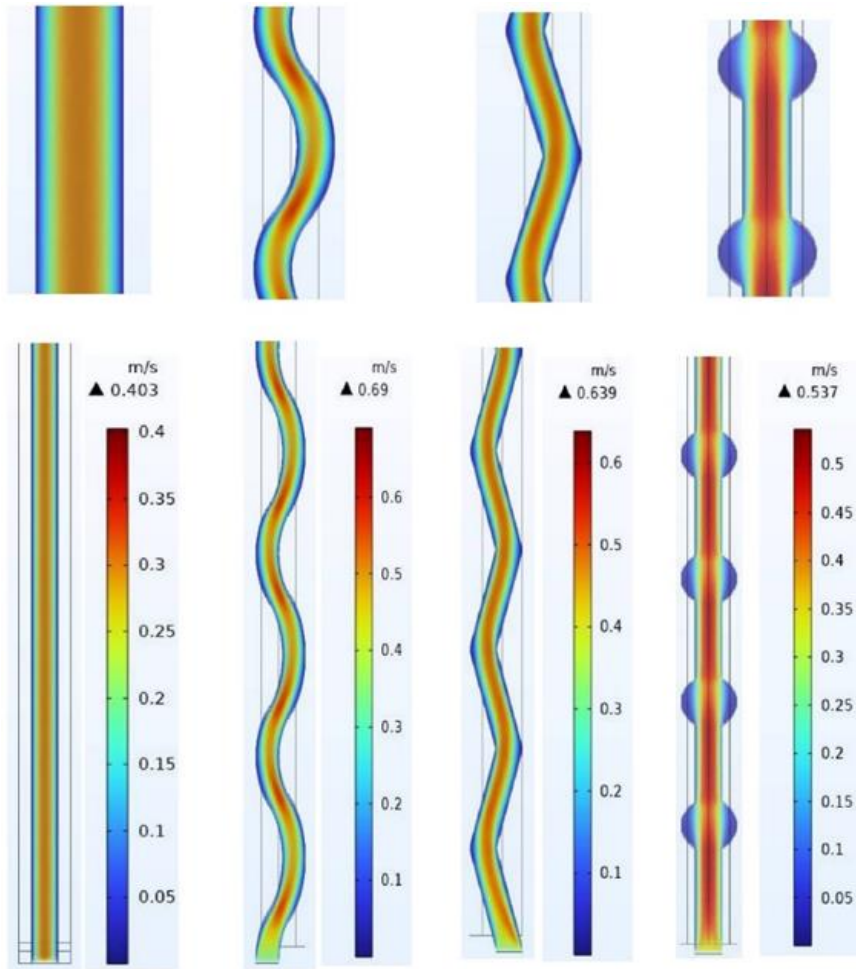
Fig. 8. Illustrates the influence of different microchannel shapes (rectangular, wavy, Zigzag, and circular cavities channel) on the velocity magnitude, using pure water as the working fluid. The Reynolds number (Re) is set at 150, and the heat flux (qw) is maintained at 170 kW/m^2

5.2 Temperature Contour Characteristics

With the aim of analyzing heat transfer and Comparison between the shapes(straight, Zigzag, wavy, and circular cavities) used in this work. Figure 9 shows the temperature distributions along the micro-channel heat sink for different types of nanofluid (Al_2O_3, CuO, and TiO_2–H_2O), and the Reynolds number (Re = 150) for pure water. The nanofluid exhibits a volume concentration of 0.01., under the same inlet conditions (T_{in} =300K). The Figure 9 Illustrates that the highest temperature is observed at the heated bottom wall of the heat sink due to the presence of heat flux. Furthermore, it should be noted that the temperature gradient increases in the y-direction as the coolant flows from the inlet to the outlet of the channel, exhibiting variations in temperature for different channel geometries. The highest temperature occurs at the outlet of the microchannel. The micro-channel heat sink exhibits its maximum heat dissipation at the inlet due to the temperature disparity between the channel and the fluid at that location. This is because the temperature of the fluid is lower than that of the channel. Convection is responsible for transmitting heat between the channel walls and the different coolants along the stream. Furthermore, the heat transfer rate exhibits a direct relationship with the thermal conductivity, density, and specific heat capacity, while it demonstrates an inverse relationship with the dynamic viscosity. The maximum temperature of the microchannel heat sink in the wavy, Zigzag, and circular cavities is higher than that of the rectangular channel.
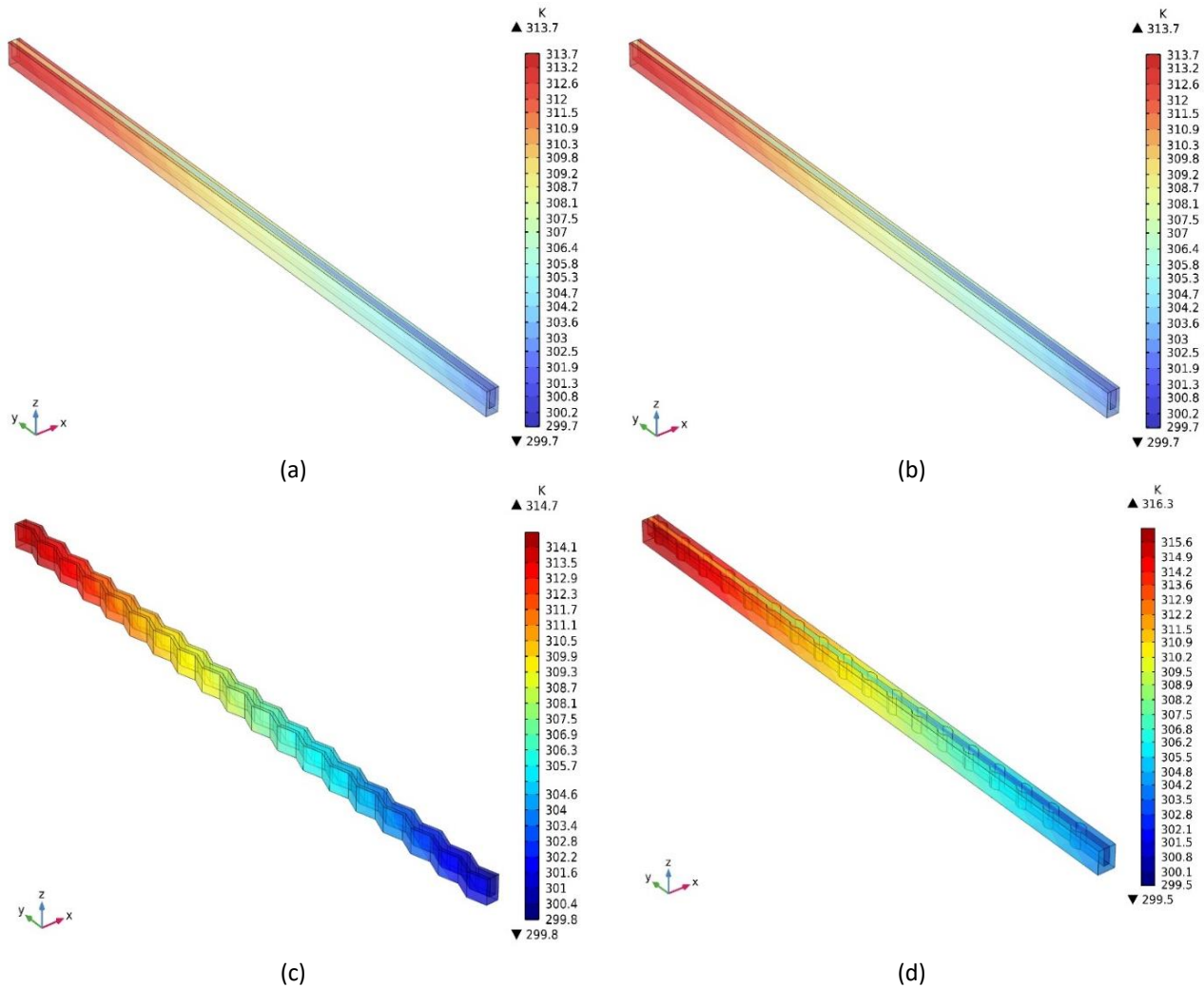
Fig. 9. Shows the temperature contour for with Pure water work fluid, Re=150, qw=170 kw/m² for the micro-channel shapes (a-straight, b-zigzag, c-wavy, and d-circular cavities)

6. The Effect of Nanofluids and Nanoparticles on Microchannel Heat Sinks

The thermal resistance of a microchannel heat sink is contingent upon both the inlet temperature of the coolant and the maximum temperature observed at the wall of the heat sink. The figures below present the thermal resistance (k/w) of the straight microchannel and different channels (zigzag, wavy, and circular cavities) studied in the search. In the range of Reynolds between 50 and 150, heat flux applied qw=(170,220,340kw/m²). And different types of (Al_2O_3, CuO ;and TiO_2–H_2O) nanofluid with a volume concentration range of(0.01, 0.02 and 0.03%). Figure 10 displays that the relationship between thermal resistance and Reynolds number (Re) is reverse proportionality. Because of the increased flow rate and the enhanced thermal dispersion effects, .thermal resistance reduces as the Reynolds number increases. The results show that the wavy microchannel has the highest thermal resistance value with (CuO) nanofluids, and lower resistance is found in the straight microchannel, with nanofluids and water as a coolant. In addition, as the proportion of nanoparticles increased, thermal resistance decreased further. The higher thermal conductivity of nanofluids might explain this reduction in thermal strength 'compared to that of pure water. A comparison of the heat transfer efficacy between a wavy and straight channels demonstrates a notable disparity.
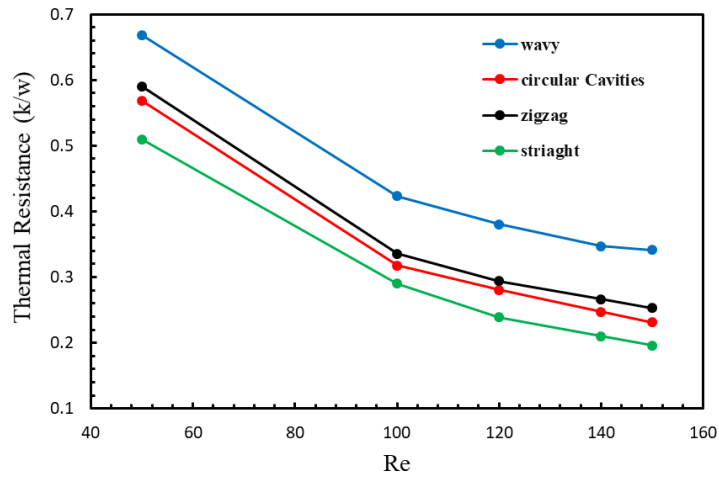
Fig. 10. shows the Thermal Resistance (k/w) of the different channels at q = 170kw/m^2 , using (0.01cuo-water)

Figure 11 below presents the straight microchannel Pressure drop ratio and different channels (zigzag, wavy, and circular cavities) studied in the search. Regardless of the channel shape, the Pressure drop increases as the Reynolds number rises. It is evident that the wavy microchannel exhibits the highest pressure drop (ΔP) among the various microchannels investigated in the current work . In addition, The more the pressure decreases as a result 'Of flux disruptions caused by variations in the orientation of the channel and secondary flow in irregular channels (zigzag, wavy, and circular cavities) used in search, as well as the contacts between vortices and the walls of the channel, heat sink pressure losses typically increase. Furthermore, the presented data below illustrates a positive correlation between increased pressure losses and enhanced heat transfer efficiency of the heat sink when employing nanofluids as opposed to the base fluid. This phenomenon can be attributed to the increased viscosity and enhanced efficiency of nanofluids.
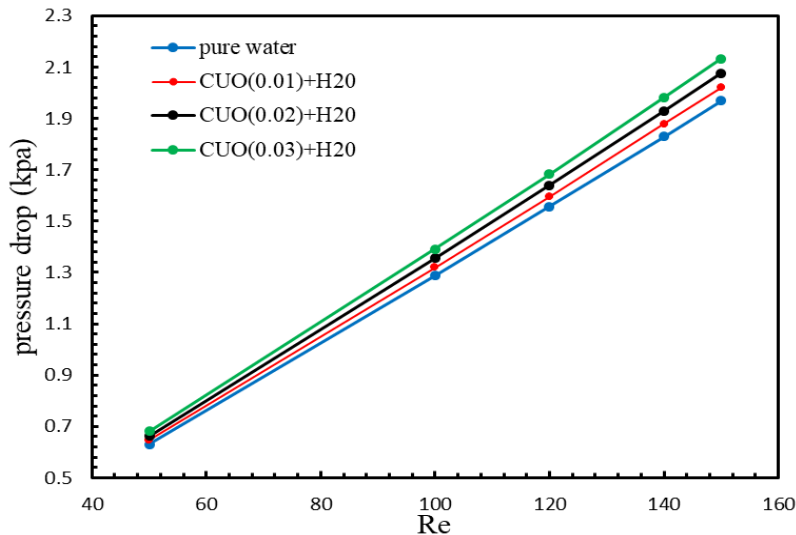
Fig. 11. illustrates the impact of utilizing a nanofluid composed of CuO-H$_2$O as a coolant on the pressure drop (ΔP) within a straight microchannel

Figure 12 below shows the friction factor's evolution with the Reynolds number for the straight microchannel and different channels (zigzag, wavy, and circular cavities) studied in the search. The

results show that the friction factor decreases as the Reynolds number (Re) increases in the various microchannels. It indicates the reversely proportional ratio of friction factor (f). The results show that the wavy microchannel has the highest friction factor, and a lower friction factor is found in the circular cavities microchannel with nanofluids and water as a coolant. Due to the flow objection with a wavy path, the high-pressure reduction causes the friction factor (f) to increase.
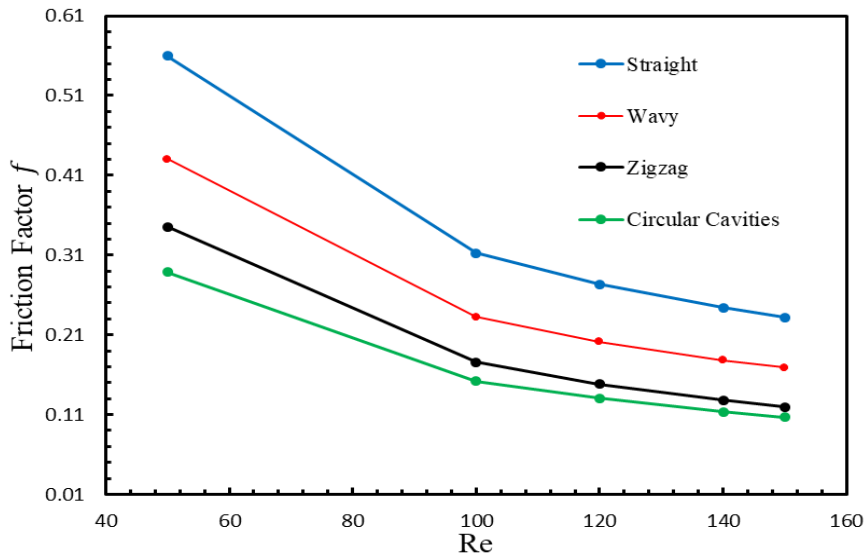
Fig. 12. Shows the effect of used (AL_2O_3-H_2O) nanofluid volume concentrations (ϕ) (0.01%) as a coolant on pressure drop (ΔP) in the different channels at q=170kw/m^2

The Figure 13 below present the Nusselt number ratio of the straight microchannel and different channels (zigzag, wavy, and circular cavities) studied in the search. In the range of Reynolds between 50 and 150, heat flux applied qw=(170,220,340 kw/m^2). And different types of (Al_2O_3, CuO, and TiO_2–H_2O) nanofluid with a volume concentration (ϕ) range of (0.01, 0.02 and 0.03%). Regardless of the channel shape, The Nusselt number rises as Reynolds' number rises. This comes at the expense of a greater pumping power Pp. The temperature gradient near the channel walls increases as the Reynolds number increases.

Contributing to increased heat transfer. Concurrently, the channel's thermal boundary layer decreases, contributing to higher heat transfer. The results showed that wavy and Zigzag geometry produced the highest Nusselt values. When cooling a heat sink using water, the Nusselt number (Nu) is lower than when utilizing nanofluids as the coolant. The Nusselt number (Nu) is higher when nanofluids are employed as coolants. This is principally because of nanofluids' increased thermal efficiency compared to the base fluid. This causes a rise 'in the heat conduction contribution to the overall energy transmission, and it rises with increasing proportion of the volume of the nanoparticles. In other words, nanofluids are more effective at transferring heat. The results obtained from the COMSOL program indicate that the heat transfer performance of wavy microchannels is higher than that of both zigzag and circular cavities, as well as straight microchannels. that the wavy microchannels can considerably improve the performance of heat transmission (CuO-H_2O) nanofluid as a coolant, and that this improvement is dependent on the mixing of fluid components within the microchannel.
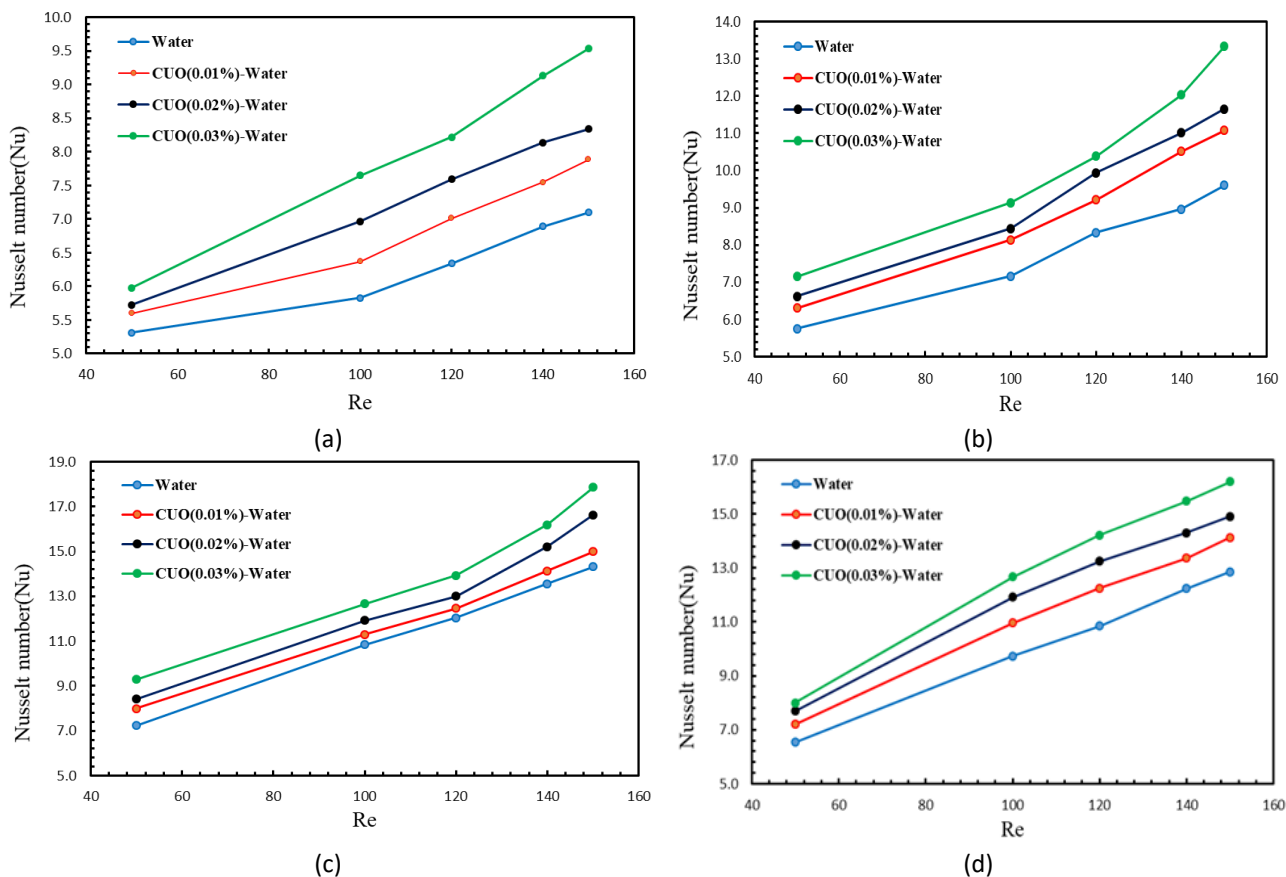
Fig. 13. Shows the effect of used (CuO-H₂O) nanofluid as a coolant on local Nusslet number(Nu) at heat flux 170kw/m² for the micro-channel shapes (a-straight, b-zigzag, c-wavy, and d-circular cavities)

7. Comparison of Experimental and Numerical Results

The obtained experimental results were then compared to the numerical results, revealing a significant level of agreement, as depicted in Figure 14. The utilization of distilled water as a coolant resulted in an error rate that varied between 1.2% and 5.2%. However, when Nanofluid was employed as a coolant, the error rate ranged from (0.75-4.9)%. Figure 15 represent the comparisons between experimental and numerical Nusselt Number (Nu) results of all channels (straight, Wavy, Zigzag and circular cavities). A similarity was observed in the general behaviour, and an apparent convergence in the results when using the Nanofluid and distilled water as a coolant, as the biggest deviation between a nusselt number values a numerical and experimental one was (2.6-9.8%). These results indicate that as flow rates increase, the wall temperature decreases while the Nusselt number rises.
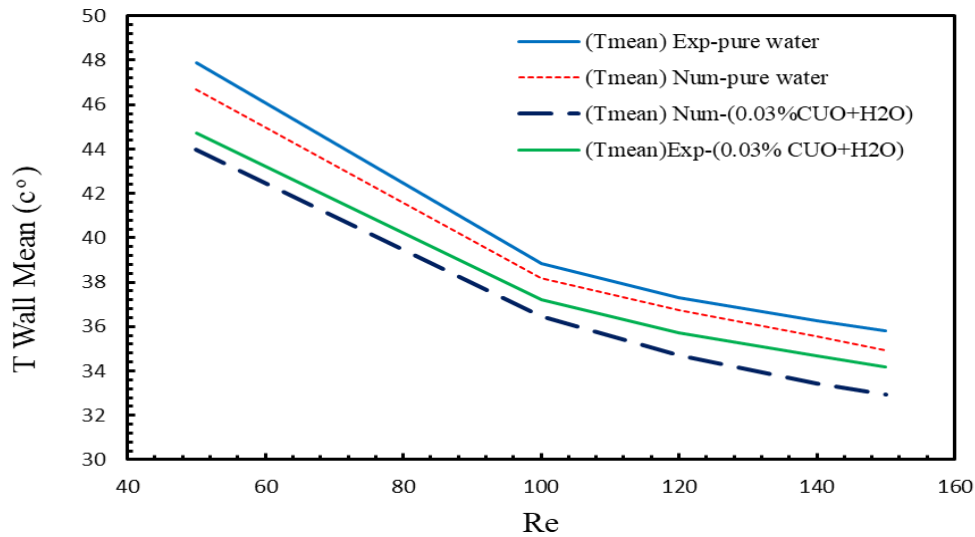
Fig. 14. shows the comparisons between numerical and experimental results of the wall temperature of the Straight microchannel heat sink
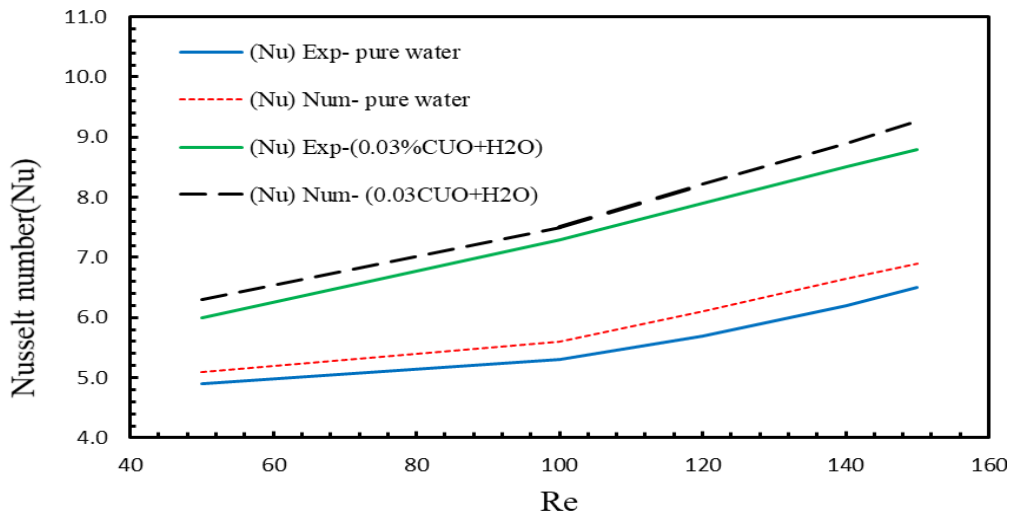
Fig. 15. Shows the comparisons between numerical and experimental results of the local Nusslet number of Straight micro-channel heat sinks

8. Conclusions

Conclusion of this research are:

i.   The results elucidated that the pressure drop increases when the geometry of the channel alters and 'with the increase of both the Reynolds number and the nanoparticle volume concentration.

ii.   The thermal resistance decreased At all values of all the Reynolds numbers and all the concentrations of nanoparticles used in the search, where the relationship is inverse with it.

iii. The findings indicated that the friction factor decreases with an increase in the Reynolds number, and it increases with As 'the volumetric concentration of nanoparticles rises.

iv.   The experimental results revealed that Nusselt's Number exhibits an upward trend as the Reynolds number increases across various channel geometries and working fluids under investigation.

v. The experimental and numerical results indicated that The findings that the mean wall temperature was found to be reduced at all the(rectangular, wavy, Zigzag, and circular cavities) microchannel heat sinks as a result of increasing the flow rate and utilizing nanofluids.

vi. The experimental and numerical results showed that the cooling performance is better for all microchannels studied in this study when using nanofluids, and it increases as 'the volumetric concentration of nanoparticles increases and at all heat flux values.

Acknowledgment

References

[1] Japar, Wan Mohd Arif Aziz, Nor Azwadi Che Sidik, R. Saidur, Natrah Kamaruzaman, Yutaka Asako, Siti Nurul Akmal Yusof, and Mohd Nizam Lani. "Hybrid Microchannel Heat Sink with Sustainable Cooling Solutions: Numerical Model Validation." *CFD Letters* 14, no. 4 (2022): 91-117. https://doi.org/10.37934/cfdl.14.4.91117

[2] Derakhshanpour, K., R. Kamali, and M. Eslami. "Improving performance of single and double-layered microchannel heat sinks by cylindrical ribs: A numerical investigation of geometric parameters." *International Communications in Heat and Mass Transfer* 126 (2021): 105440. https://doi.org/10.1016/j.icheatmasstransfer.2021.105440

[3] Dąbrowski, Paweł. "Thermohydraulic maldistribution reduction in mini heat exchangers." *Applied Thermal Engineering* 173 (2020): 115271. https://doi.org/10.1016/j.applthermaleng.2020.115271

[4] Farsad, E., S. P. Abbasi, M. S. Zabihi, and J. Sabbaghzadeh. "Numerical simulation of heat transfer in a micro channel heat sinks using nanofluids." *Heat and mass transfer* 47, no. 4 (2011): 479-490. https://doi.org/10.1007/s00231-010-0735-y

[5] Sidik, Nor Azwadi Che, Muhammad Noor Afiq Witri Muhamad, Wan Mohd Arif Aziz Japar, and Zainudin A. Rasid. "An overview of passive techniques for heat transfer augmentation in microchannel heat sink." *International Communications in Heat and Mass Transfer* 88 (2017): 74-83. http://dx.doi.org/10.1016/j.icheatmasstransfer.2017.08.009

[6] Kamaruzaman, Natrah, Mohd Farhan Wisley, Ummikalsom Abidin, Mohsin Mohd Sies, and Mohd Ridhwan Mohd Ruslan. "Effect of Channel Arrangement on the Thermal Hydraulic Performance of Multilayer Microchannel Arrays." *CFD Letters* 12, no. 8 (2020): 17-25. https://doi.org/10.37934/cfdl.12.8.1725

[7] Manshoor, Bukhari, Azwan Sapit, Normayati Nordin, Azian Hariri, Hamidon Salleh, Mohd Azahari Razali, Izzuddin Zaman, Amir Khalid, Mohd Fairusham Ghazali, and Muneer Khalifa Alsayed. "Simulation of fractal like branching microchannel network on rectangular heat sink for single phase flow." *CFD Letters* 12, no. 2 (2020): 69-79.

[8] Hodes, Marc, Randy D. Weinstein, Stephen J. Pence, Jason M. Piccini, Lou Manzione, and Calvin Chen. "Transient thermal management of a handset using phase change material (PCM)." *J. Electron. Packag.* 124, no. 4 (2002): 419-426. https://doi.org/10.1115/1.1523061

[9] Kim, Seo Young, Jin Wook Paek, and Byung Ha Kang. "Thermal performance of aluminum-foam heat sinks by forced air cooling." *IEEE Transactions on components and packaging technologies* 26, no. 1 (2003): 262-267. https://doi.org/10.1109/TCAPT.2003.809540

[10] Shabgard, Hamidreza, Michael J. Allen, Nourouddin Sharifi, Steven P. Benn, Amir Faghri, and Theodore L. Bergman. "Heat pipe heat exchangers and heat sinks: Opportunities, challenges, applications, analysis, and state of the art." *International Journal of Heat and Mass Transfer* 89 (2015): 138-158. https://doi.org/10.1016/j.ijheatmasstransfer.2015.05.020

[11] Kandasamy, Ravi, Xiang-Qi Wang, and Arun S. Mujumdar. "Transient cooling of electronics using phase change material (PCM)-based heat sinks." *Applied thermal engineering* 28, no. 8-9 (2008): 1047-1057. https://doi.org/10.1016/j.applthermaleng.2007.06.010

[12] Mudawar, Issam. "Assessment of high-heat-flux thermal management schemes." *IEEE transactions on components and packaging technologies* 24, no. 2 (2001): 122-141. https://doi.org/10.1109/6144.926375

[13] Gujarathi, Harshal. "Use of nanoparticle enhanced phase change material (nepcm) for data center cooling application." (2014). http://hdl.handle.net/10106/26707

[14] Muhammad, Nura Mu'az, Nor Azwadi Che Sidik, Aminuddin Saat, and Bala Abdullahi. "Effect of nanofluids on heat transfer and pressure drop characteristics of diverging-converging minichannel heat sink." *CFD Letters* 11, no. 4 (2019): 105-120.

[15] Zheng, Dan, Jin Wang, Zhanxiu Chen, Jakov Baleta, and Bengt Sundén. "Performance analysis of a plate heat exchanger using various nanofluids." *International Journal of Heat and Mass Transfer* 158 (2020): 119993. https://doi.org/10.1016/j.ijheatmasstransfer.2020.119993

[16] Sakanova, Assel, Chan Chun Keian, and Jiyun Zhao. "Performance improvements of microchannel heat sink using wavy channel and nanofluids." *International journal of heat and mass transfer* 89 (2015): 59-74. https://doi.org/10.1016/j.ijheatmasstransfer.2015.05.033

[17] Nitiapiruk, Piyanut, Omid Mahian, Ahmet Selim Dalkilic, and Somchai Wongwises. "Performance characteristics of a microchannel heat sink using TiO2/water nanofluid and different thermophysical models." *International Communications in Heat and Mass Transfer* 47 (2013): 98-104. https://doi.org/10.1016/j.icheatmasstransfer.2013.07.001

[18] Feng, Zhenfei, Xiaoping Luo, Feng Guo, Haiyan Li, and Jinxin Zhang. "Numerical investigation on laminar flow and heat transfer in rectangular microchannel heat sink with wire coil inserts." *Applied Thermal Engineering* 116 (2017): 597-609. https://doi.org/10.1016/j.applthermaleng.2017.01.091

[19] Mala, Gh Mohiuddin, and Dongqing Li. "Flow characteristics of water in microtubes." *International journal of heat and fluid flow* 20, no. 2 (1999): 142-148. https://doi.org/10.1016/S0142-727X(98)10043-7

[20] Papanastasiou, Tasos, Georgios Georgiou, and Andreas N. Alexandrou. *Viscous fluid flow*. CRC press, 2021. https://doi.org/10.1201/9780367802424

[21] Japar, Wan Mohd Arif Aziz, Nor Azwadi Che Sidik, R. Saidur, Natrah Kamaruzaman, Yutaka Asako, Siti Nurul Akmal Yusof, and Mohd Nizam Lani. "Hybrid Microchannel Heat Sink with Sustainable Cooling Solutions: Numerical Model Validation." *CFD Letters* 14, no. 4 (2022): 91-117. https://doi.org/10.37934/cfdl.14.4.91117

[22] Kumar, D. Sathish, and Somasundaram Jayavel. "FLOW AND HEAT TRANSFER ANALYSIS OF MICROCHANNEL HEAT SINK WITH SOLID INSERTS FOR ELECTRONIC COOLING APPLICATIONS." *Heat Transfer Research* 54, no. 17 (2023). https://doi.org/10.1615/HeatTransRes.2023048353

[23] Japar, Wan Mohd Arif Aziz, Nor Azwadi Che Sidik, Rahman Saidur, Natrah Kamaruzaman, Yutaka Asako, and Siti Nurul Akmal Yusof. "The effect of triangular cavity shape on the hybrid microchannel heat sink performance." *CFD Letters* 12, no. 9 (2020): 1-14. https://doi.org/10.37934/cfdl.12.9.114

[24] Sadaghiani, Abdolali K. "Numerical and experimental studies on flow condensation in hydrophilic microtubes." *Applied Thermal Engineering* 197 (2021): 117359. https://doi.org/10.1016/j.applthermaleng.2021.117359

[25] Japar, Wan Mohd Arif Aziz, Nor Azwadi Che Sidik, R. Saidur, Natrah Kamaruzaman, Yutaka Asako, Siti Nurul Akmal Yusof, and Mohd Nizam Lani. "Hybrid Microchannel Heat Sink with Sustainable Cooling Solutions: Experimental Analysis." *Journal of Advanced Research in Applied Mechanics* 89, no. 1 (2022): 1-6. https://doi.org/10.37934/aram.89.1.16

[26] Yuan, Jin, Yongfeng Qu, Ningkang Deng, Liang Du, Wenbo Hu, Xiaofan Zhang, Shengli Wu, and Hongxing Wang. "Three-dimensional numerical investigation of flow and heat transfer performances of novel straight microchannel heat sinks." *Diamond and Related Materials* 140 (2023): 110479. https://doi.org/10.1016/j.diamond.2023.110479